Structural relationships between non-crystalline phases in AlMn and AlFeCr systems through EXAFS measurements

1989 J. Phys.: Condens. Matter 1 4283

(http://iopscience.iop.org/0953-8984/1/27/002)

J. Phys.: Condens. Matter **1** (1989) 4283–4296. Printed in the UK

Structural relationships between non-crystalline phases in AlMn and AlFeCr systems through EXAFS measurements

A Sadoc† and J M Dubois‡

† LURE bat. 209D, Université Paris-Sud, 91405, Orsay Cédex, France

‡ Laboratoire de Sciences et Génie des Matériaux Métalliques, Ecole des Mines, Parc de Saurupt, 54042 Nancy Cédex, France

Received 1 March 1988, in final form 23 November 1988

Abstract. We report EXAFS experiments above the Mn K absorption edge in decagonal, icosahedral and amorphous phases of AlMn alloys and above the Fe and Cr edges in decagonal and icosahedral AlFeCr alloys. In icosahedral phases, the first shell of neighbours surrounding a Mn/Fe/Cr atom has been interpreted starting from a Mackay icosahedron modelling. For AlMn alloys, a relationship between nearest Mn–Mn pairs and magnetism results is suggested.

1. Introduction

The icosahedral quasi-crystalline phase formed in Al–Mn alloys by rapid quenching of the melt is metastable (Shechtman *et al* 1984). When the solidification conditions are less rapid, another metastable quasi-crystal (decagonal phase; Bendersky 1985) or equilibrium crystalline phases can be obtained. Recently, amorphous aluminium–transition metal alloys were prepared, and possible structural resemblances between icosahedral and decagonal phases (Bendersky *et al* 1985) or between amorphous and icosahedral phases (Dubois *et al* 1985, 1987, Boyce *et al* 1986) are suggested.

To elucidate further the nature of the local structure in the non-crystalline phases, we have performed EXAFS (extended x-ray absorption fine structure) measurements in amorphous, icosahedral and decagonal AlMn alloys as well as in icosahedral and decagonal AlFeCr alloys. Preliminary results have been recently published (Sadoc *et al* 1988b); our findings are compared with recent neutron diffraction data obtained by isomorphous substitution (Dubois and Janot 1987, 1988, Janot *et al* 1987a). Moreover, in the case of the AlMn system, the possible interrelationships between the local order and magnetic behaviour are investigated.

2. Experimental details

The samples were obtained from different sources. Rapidly quenched ribbons of decagonal $Al_{80}Mn_{20}$ (T-AlMn) and $Al_{80}(Cr_{0.5}Fe_{0.5})_{20}$ (T-AlFeCr) and of icosahedral $Al_{86}Mn_{14}$ (i-AlMn) and $Al_{82}Si_1(Fe_{0.5}Cr_{0.5})_{17}$ (i-AlFeCr) were produced by melt spinning. The

0953-8984/89/274283 + 14 $02.50

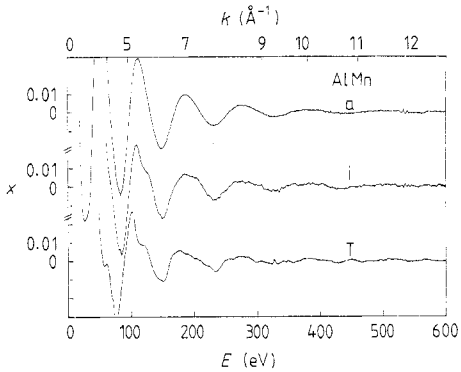

Figure 1. Experimental EXAFS spectra above the Mn K edge in amorphous (a), icosahedral (i) and decagonal (T) AlMn alloys.

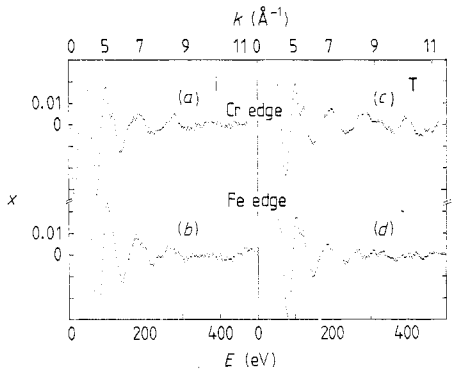

Figure 2. Experimental EXAFS spectra above the Cr (top: (*a*), (*c*)) and Fe (below (*b*), (*d*)) K edges in icosahedral ((*a*), (*b*)) and decagonal ((*c*), (*d*)) AlFeCr alloys.

decagonal phases and the icosahedral AlFeCr sample were prepared in the Laboratoire de Sciences et Génie des Matériaux Métalliques (Ecole des Mines, Nancy, France). The icosahedral $Al_{86}Mn_{14}$ sample was obtained from G Regazzoni and R Rey-Flandrin (Péchiney, Voreppe, France). The icosahedral samples contained about 10% of FCC Al while the decagonal phases were obtained as single phases. The amorphous ribbon (a-AlMn) was prepared by sputtering from an $Al_{85}Mn_{15}$ alloy (CRTBT, Grenoble, France). Moreover, two crystalline samples, o-Al_6Mn and α-AlMnSi, were used for comparison. The orthorhombic phase o-Al_6Mn was prepared by annealing at 640 °C an $Al_{86}Mn_{14}$ alloy (LEPES, Grenoble, France). The α-AlMnSi phase was obtained from an $Al_{73}Mn_{16}Si_{11}$ alloy by annealing at 500 °C (CECM, Vitry, France). A few per cent of FCC Al (1–2%) was present in the sample. The samples were characterised by x-ray or neutron diffraction. They were studied in the ribbon shape, except for the crystalline alloys and for i-AlFeCr which were in powder form. In this last case, the powders were ground by hand, sieved through a 50 μm mesh and rubbed onto Scotch transparent tape; several layers were used in order to achieve a K-edge jump of $\Delta\mu \simeq 1$.

The EXAFS experiments were carried out at LURE (Orsay) using DCI synchrotron radiation. They were performed at 25 K on experimental station EXAFS 3 using a Si(311) double-crystal monochromator and on the EXAFS 1 spectrometer using a Si(331) channel cut monochromator. The K absorption edges of Cr (5988 eV), Mn (6540 eV) and Fe (7112 eV) were investigated. As reference samples and for energy calibration chromium, manganese and iron metal foils were used.

3. EXAFS analysis

The EXAFS oscillations $\chi(E)$ were obtained by standard analytical procedures and are shown in figures 1 and 2. The signal is more structured in AlFeCr alloys than in the AlMn ones, a fact which was also encountered in the AlMnCr system (Sadoc 1986) and which goes along with the more rapid damping of the oscillations of total pair correlation functions in AlMn alloys than in AlFeCr ones (Dubois and Janot 1987). The magnitudes

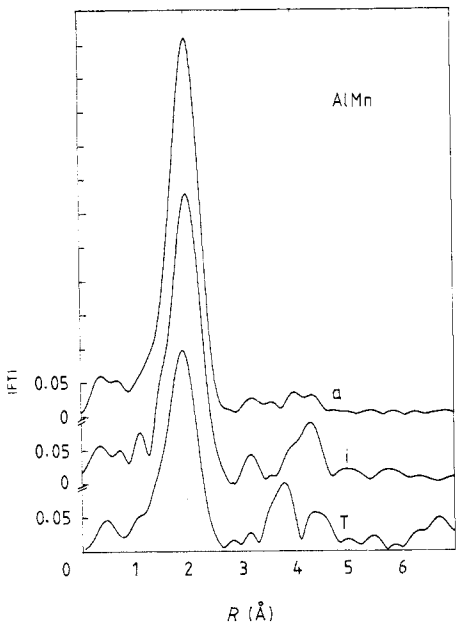

Figure 3. AlMn alloys: Fourier transform of $k^3\chi(k)$ on the Mn K edge for amorphous (a), icosahedral (i) and decagonal (T) AlMn alloys.

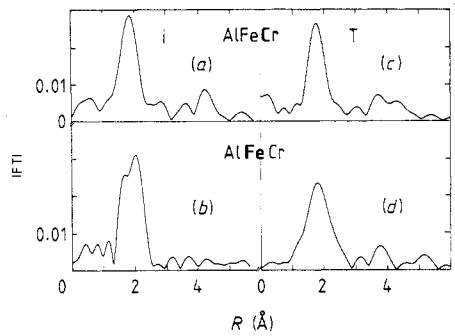

Figure 4. AlFeCr alloys: Fourier transform of $k^3\chi(k)$ on the Cr (top: (*a*), (*c*)) and Fe (below: (*b*), (*d*)) K edges in icosahedral ((*a*), (*b*)) and decagonal ((*c*), (*d*)) phases.

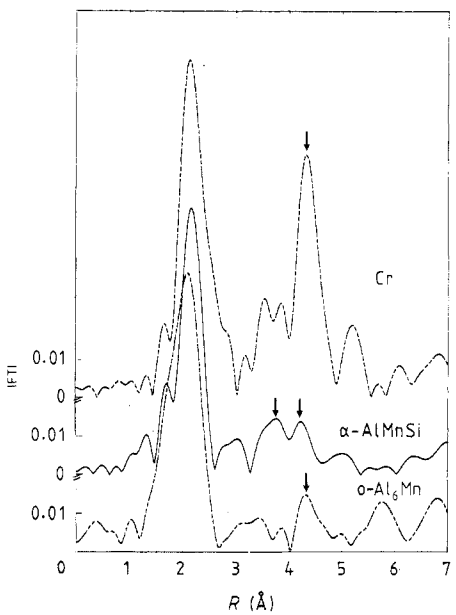

Figure 5. Fourier transform of $k^3\chi(k)$ on the Cr K edge in chromium, and on the Mn K edge in α-AlMnSi and in o-Al_6Mn. The arrows indicate the peaks used in the EXAFS analysis.

of the Fourier transforms (FT) of $k^3\chi(k)$ are given in figures 3, 4 and 5 for the various samples. These FT are related to the average radial distribution functions (RDF) of the atoms neighbouring the absorbing atom (Cr, Mn or Fe). The peaks are shifted to lower

R because of the phase shifts experienced by the photoelectron while scattering from the potentials of the absorbing atom and nearest neighbours.

The FT display a main peak at about 2 Å, due to first neighbours, and some secondary peaks at higher R. Although the position of the first-neighbour peak does not change much through the quasi-crystalline samples, the existence and the location of the peaks in the vicinity of 4 Å vary drastically from one sample to another. We will try to elucidate these structures in the following.

For amorphous a-AlMn, the FT displays only one first-neighbour peak due to disorder-induced broadening of the distribution of secondary and higher neighbour distances; the amplitude of this peak is, however, larger than for the quasi-crystalline phases. For icosahedral and decagonal AlMn alloys, the peaks at 4.3 Å have their counterpart in the FT of the α-AlMnSi and o-Al_6Mn spectra (figure 5). On the other hand, the peak at 3.7 Å in the decagonal phase appears only as a small wing in i-AlMn (figure 3). However, it has its fellow in the FT of α-AlMnSi (figure 5). This result suggests that the structure of the T-phase, a two-dimensional quasi-crystal, is intermediate between the α and the i phases.

Looking now at the AlFeCr system, the FT for the icosahedral alloy displays a remarkable peak at 4.2 Å but only on the Cr edge (figure 4*a*). This peak was already encountered for the icosahedral $Al_{86}Cr_{14}$ alloy (Sadoc *et al* 1987) and was found to be due to Cr–Cr correlations by comparison with pure chromium (figure 5). On the Fe edge (figure 4*b*), the FT does not display any second or higher correlation peaks. At last, the decagonal AlFeCr phase displays, on both Fe and Cr edges (figures 4*c*, *d*), a peak at 3.7 Å as in decagonal AlMn alloy. In addition, the FT on the Cr edge shows some structure at about 4.2 Å (figure 4*c*). Therefore, the second and higher neighbours look quite different around a Fe or a Cr atom in both icosahedral and decagonal AlFeCr phases.

To compare quantitatively the different phases, the main peaks were back-Fourier-transformed to k space. Analysis of the k-dependence of the back-transforms of the second and third shells shows that the relevant EXAFS signal is mostly the result of backscattering by heavy elements—therefore Mn or Fe/Cr atoms—and that the backscattering by Al atoms has little influence on it. The inverse FT of the peaks at 3.7 Å in T-AlMn, T-AlFeCr on the Fe edge and in α-AlMnSi were found in phase, and so it was for the peaks at 4.3 Å in T-AlMn and in o-Al_6Mn. The same holds true also for the inverse FT of the peaks at 4.2 Å in i-AlFeCr on the Cr edge and in pure chromium.

Therefore, the Fourier-filtered EXAFS were calculated using the following formula (Stern *et al* 1975) which, in single-scattering theories and in the plane-wave approximation, described the EXAFS oscillations for Gaussian distributions of neighbours around a central atom:

$$\chi(k) = -\sum_j (N_j/kR_j^2)|f_j(\pi)| \exp[-2\sigma_j^2 k^2 - (2R_j/\lambda)] \sin\{2kR_j + 2\delta_1' + \arg(f_j(\pi))\}.$$

The sum is taken over shells with N_j atoms at distances R_j from the absorbing atom. The Debye–Waller factor $\exp(-2\sigma_j^2 k^2)$ is a measure of the disorder in shell j. It arises mainly from structural disorder since the experiments were made at low temperatures. The photoelectron wavevector k is related to the photon energy E by $k = [2m(E - E_0)/\hbar^2]^{1/2}$, where E_0 is the threshold energy, $f_j(\pi)$ is the backscattering amplitude for the photoelectron by the neighbours, and δ_1' is the phase shift of the central atom. $\lambda(k)$ is the electron mean free path and is taken to be of the form k/Γ (Lee and Pendry 1975), where Γ is a constant that has been determined in reference materials

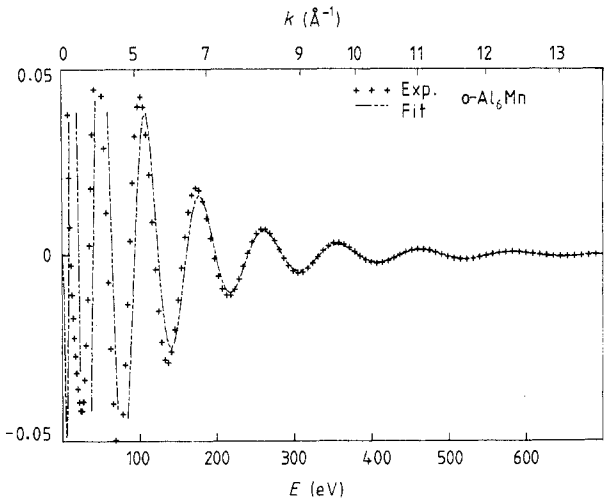

Figure 6. o-Al_6Mn: Fourier-filtered first peak of the FT on the Mn K edge (full curve) and its reconstruction (broken curve) using crystallographic data.

($\Gamma = 0.80$, 0.85 and 0.55 $Å^{-2}$ for Cr, Mn and Fe, respectively). The backscattering amplitudes and phase shifts for Al on the one hand, and the central atom phase shifts for Cr, Mn and Fe on the other, were respectively taken from Lee and Beni (1977) and from Teo and Lee (1979) as they have been checked in previous studies (Fontaine *et al* 1979, Sadoc *et al* 1986, 1987). For Mn–Mn and Cr–Cr pairs, experimental amplitudes and phase shifts were extracted from the crystalline references, o-Al_6Mn, α-AlMnSi and pure chromium, the structure of which will be briefly described in § 4.

4. Crystalline reference structures

4.1. o-Al_6Mn

The orthorhombic structure of Al_6Mn has been determined by Nicol (1953). The space group is D_{2h}^{17}-Ccmm. Each Mn atom has ten nearest Al atoms (two at 2.435 Å, two at 2.54 Å, four at 2.60 Å and two at 2.64 Å). Using these crystallographic data, the inverse FT of the first-neighbour peak of Al_6Mn has been well reconstructed with $\sigma = 0.07$–0.08 Å and $\Gamma = 0.85$ $Å^{-2}$ (figure 6). As for the Mn–Mn shortest distances, they are 4.475 Å (2 Mn) and 4.985 Å (4 Mn) and both contributions are mixed in the peak at 4.3 Å in the FT (figure 5). Therefore, experimental amplitudes and phase shifts were extracted from the peak using six Mn atoms at an average distance $\bar{R} = 4.815$ Å and assuming that the contributions of Al second or further neighbours are negligible compared with those of Mn.

4.2. α-AlMnSi

The structure of the α-AlMnSi phase (space group Pm3, $a = 12.56$ Å) has been determined by Cooper and Robinson (1966). There are two types of Mn atom sites, Mn(1)

and Mn(2). All Mn atoms are surrounded by Al atoms and there are no Mn–Mn first neighbours. Taking 2.84 Å as the maximum contact distance for manganese and aluminium atoms, Mn(1) have ten Al neighbours and Mn(2) nine Al ones; the 12 different Mn–Al distances range from 2.27 Å to 2.84 Å, with a mean $\bar{R} = 2.59$ Å. The peaks at 3.7 Å and 4.2 Å in the FT (figure 5) correspond to the Mn–Mn shortest distances, five Mn between 4.385 Å and 4.55 Å, and five Mn between 4.85 Å and 5.125 Å. Experimental amplitudes and phase shifts were extracted from these peaks using five Mn at an average distance $\bar{R} = 4.46$ Å for the second peak and five Mn at $\bar{R} = 5.04$ Å for the third peak.

4.3. Cr structure

Chromium has a body-centred cubic BCC structure (Wyckoff 1982). Each atom is surrounded by eight first neighbours at the centres of surrounding cubes (2.50 Å), six atoms at the corners of adjacent cubes (2.88 Å), 12 along the [110] axes (4.08 Å), 24 at $a\sqrt{11}/2$ (4.78 Å) and eight along the [111] axes (5.00 Å).

The contributions due to first and second neighbours were found to be mixed in the main FT peak (figure 5). The peak at 4.20 Å is due principally to the 24 fourth neighbours at 4.78 Å. Some contributions come, however, from the fifth shell of eight Cr atoms at 5.00 Å. Therefore, experimental amplitudes and phase shifts were extracted from the inverse FT of the peak at 4.2 Å using 32 atoms at $\bar{R} = 4.835$ Å.

5. Al–Mn system

5.1. Icosahedral $Al_{86}Mn_{14}$

The results for i-AlMn have already been reported (Sadoc *et al* 1986, Sadoc 1986) and will be only summarised here. The inverse FT of the first peak was interpreted using a Mackay icosahedron modelling with the aim of testing the model proposed by Audier and Guyot (1986) who constructed the AlMn quasi-crystals starting from a BCC packing of Mackay icosahedra (MI) (Mackay 1962). In this model, the basic unit is a double icosahedron and the icosahedra are connected in parallel orientation along the 3-fold axes by octahedral Mn bonds. The Mn atoms are located at the vertices of an icosahedron, the centre of which is unoccupied (figure 7); 12 Al atoms are at half the distance of the vectors pointing to the Mn vertices, thereby forming a half-sized parallel icosahedron. Moreover, 30 Al atoms are near the mid-points of the edges of the larger Mn icosahedron forming an icosidodecahedron.

With the MI description, a Mn atom is surrounded by one Al at 2.425 Å plus five Al at 2.55 Å which belong to the same MI as the central atom. We have shown that more distant subshells are necessary to reconstruct the EXAFS signal: about three Al at ~2.72 Å have to be added or two Al at this distance plus 0.5–1 Mn at ~2.62 Å. The results are reported in table 1. Therefore, the MI model cannot describe satisfactorily the icosahedral structure. This is consistent with the conclusions drawn recently by several workers, revealing either that relatively few complete Mackay icosahedra exist (Janot *et al* 1988, Cahn *et al* 1988, Gratias 1988), or that only part of the atoms are members of MIS (Duneau and Oguey 1989). The Mn–Al radial distribution (figure 8) shows an asymmetry towards large distances. This was also found in i-AlMnSi by EXAFS (Sadoc *et al* 1988a) and by neutron diffraction (Dubois *et al* 1988). This is a remarkable feature since in the crys-

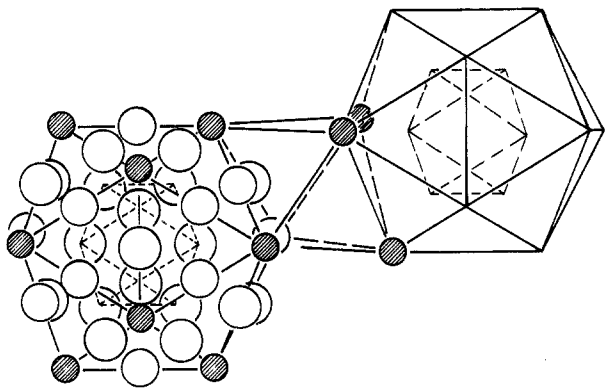

Figure 7. Mackay icosahedron. The small shaded circles represent the transition metal atoms (Mn/Fe/Cr) and the big circles are the Al atoms.

Table 1. Structural parameters for decagonal, icosahedral and amorphous AlMn and AlFeCr alloys. $\Delta R = \pm 0.05$ Å, $\Delta\sigma = \pm 0.01$ Å, for the first shell $\Delta N = \pm 0.5$ at., and for further shells $\Delta N = \pm 1$ at.

Central atom	Decagonal $Al_{80}Mn_{20}$ N	R (Å)	σ (Å)	Icosahedral $Al_{86}Mn_{14}$ N	R (Å)	σ (Å)	Amorphous $Al_{85}Mn_{15}$ N	R (Å)	σ (Å)
				1 Al	2.425	0.08			
	6.2 Al	2.54	0.11	5 Al	2.55	0.09	9.5 Al	2.515	0.113
	2.5 Al	2.71	0.13	2–3 Al	2.72	0.15			
Mn	0.5 Mn	2.58	0.12	0.5–1 Mn	2.62	0.11	0.5 Mn	2.62	0.13
	5 Mn	4.47	$\delta\sigma = 0.05$	3 Mn	4.5	$\delta\sigma = 0.05$			
	5 Mn	4.77	$\delta\sigma = 0.06$	3–7 Mn	4.7	$\delta\sigma = 0.06$			
				(3 Mn	4.9	$\delta\sigma = 0.06$)			
	$Al_{80}(Cr_{0.5}Fe_{0.5})_{20}$			$Al_{82}Si_1(Cr_{0.5}Fe_{0.5})_{17}$					
				1 Al	2.48	0.09			
	6 Al	2.53	0.13	5 Al	2.58	0.11			
Fe	4 Al	2.80	0.17	3–4 Al	2.77	0.15			
	0.5 Fe/Cr	2.61	0.14	0.5 Fe/Cr	2.60	0.12			
	3 Fe/Cr	4.47	$\delta\sigma = 0.05$						
				1 Al	2.48	0.08			
	6 Al	2.53	0.11	5 Al	2.58	0.10			
Cr	4 Al	2.80	0.12	3–4 Al	2.77	0.15			
	0.5 Fe/Cr	2.61	0.11	0.5 Fe/Cr	2.60	0.12			
	4 Fe/Cr	4.5	$\delta\sigma = 0.06$	3 Fe/Cr	4.45	$\delta\sigma = 0.08$			
	2 Fe/Cr	4.87	$\delta\sigma = 0.05$	3.5 Fe/Cr	4.87	$\delta\sigma = 0.04$			
	4 Fe/Cr	5.0	$\delta\sigma = 0.032$	4 Fe/Cr	5.1	$\delta\sigma = 0.05$			

talline phases, o-Al_6Mn and α-AlMnSi, the asymmetry of the Mn–Al distribution is towards small distances.

EXAFS has first shown the possible existence of some Mn–Mn nearest-neighbour pairs (Sadoc *et al* 1986), which may give a structural origin to the particular magnetic properties

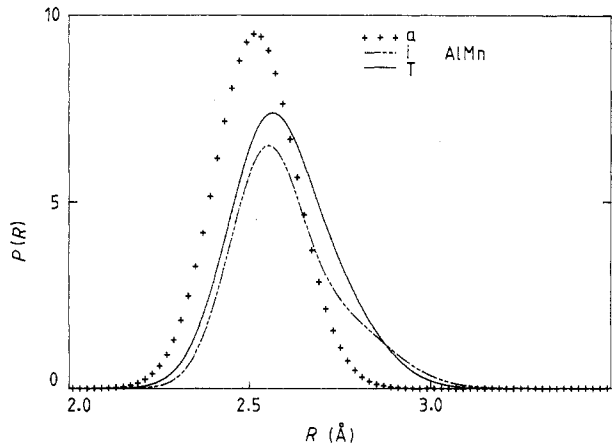

Figure 8. Mn–Al pair distribution function in amorphous (a: crosses), icosahedral (i: broken curve) and decagonal (T: full curve) AlMn alloys.

later observed in the i-AlMn alloy. We find 0.5–1 Mn nearest neighbour from a Mn atom. The same figure was obtained in i-$Al_{73}Mn_{21}Si_6$ where 0.5–1 Mn were found in the first coordination shell of a Mn atom (Sadoc *et al* 1988). A similar result was found by neutron diffraction in icosahedral $Al_{74}Mn_{21}Si_5$ (Dubois *et al* 1988) as well as in liquid AlMn alloys (Maret *et al* 1988). At this point, we may only mention that these data were found consistent with the small fraction of magnetic Mn atoms obtained by recent magnetisation studies in icosahedral AlMn and AlMnSi alloys (Bellissent *et al* 1987, Lasjaunias *et al* 1987, Berger *et al* 1988a).

The peak in the vicinity of 4 Å is due to Mn atoms at 4.73 Å with some Mn contributions at 4.5 Å and 4.9 Å. For the simulations of this multi-component peak, the estimated errors are $\Delta N = \pm 1$ at. and $\Delta R = \pm 0.1$ Å. In their EXAFS study of i-$Al_{84.6}Mn_{15.4}$, Ma *et al* (1986) noted that the FT shows only two of the first three distinct peaks of i-$Al_{79}Mn_{15.4}Si_{5.6}$, and they interpreted the peak at 4.3 Å by 4.8 ± 0.5 Mn at an average distance of 4.95 ± 0.05 Å.

5.2. *Amorphous $Al_{85}Mn_{15}$*

The inverse FT of the main peak is very similar to those obtained for icosahedral AlMn. It can be reconstructed using 9.5 Al at 2.515 Å and 0.5 Mn at 2.62 Å (table 1). The Mn–Al distribution is not asymmetrical contrary to the one in i-AlMn (figure 8), indicating that the amorphous phase has fewer Al neighbours at greater distances. The same qualitative result was obtained by Boyce *et al* (1986), who assumed only Al first neighbours in their EXAFS analysis.

On the other hand, our EXAFS results yield less than 1% of Mn–Mn first neighbours in the alloy, which compares well with magnetic results achieved by Berger *et al* (1988b) in the same a-$Al_{85}Mn_{15}$ sample. In fact, they found a small fraction of Mn magnetic atoms in the amorphous phase than in the i-phase (0.7% against 3–5%), but the actual Mn concentration in the amorphous sample is 15%, whereas it must be higher in the icosahedral one due to the presence of residual FCC Al. Moreover, the percentage of

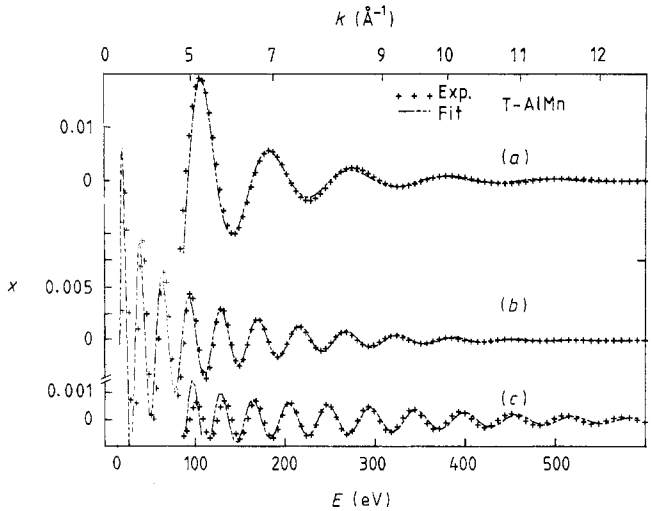

Figure 9. T–AlMn alloy: Fourier-filtered first (*a*), second (*b*) and third shell (*c*) on the Mn K edge (crosses) and their simulation (dashed line) as described in the text.

Mn–Mn pairs appears even smaller than in the case of a random distribution of atoms (1.5%), indicating a chemical ordering between unlike pairs such as Mn–Al.

A possible interpretation of the origin of magnetism in icosahedral AlMn and AlMnSi or in amorphous AlMn alloys phase is to assign it to the existence of one Mn–Mn close contact distance. However, Mn atoms in hexagonal β-Al_9Mn_3Si (Robinson 1952) have two neighbours at 2.67 Å, but carry no moment. Therefore, supplementary conditions are required to explain the magnetic ordering. It could be related to the particular fivefold symmetry that exists in quasi-crystals and also, locally, in amorphous phase and may induce the formation of specific Mn coordination that cannot occur in crystals.

5.3. Decagonal T-Al_4Mn

The inverse FT of the first-neighbour peak has been fitted with 6.2 Al at 2.54 Å plus 2.5 Al at 2.71 Å and 0.5 Mn at 2.58 Å (figure 9*a*). The Mn–Al radial distribution of the Al pairs around a Mn atom is shown in figure 8 and resembles those obtained for i-AlMn. There is a total of about 9 ± 1 Al at an average distance $\bar{R} = 2.56$ Å, taking into account the different σ parameters of the Gaussian distributions. This result compares well with recent data obtained by neutron diffraction using contrast variation techniques (Dubois and Janot 1988, Janot *et al* 1987a, b). They have found 10.4 Al at 2.55 Å and 0.3 Mn at 2.6 Å around a Mn atom.

The inverse FT of the secondary peak at 3.7 Å, which was found in phase with the corresponding peak in α-AlMnSi, was fitted using experimental amplitudes and phase shifts extracted from this peak in α-AlMnSi. It was reconstructed using 5 Mn at 4.47 Å (figure 9*b*). Once again, this result is consistent with those of Janot *et al* (1987a), i.e., 5.1 Mn at 4.5 Å.

Finally, we have tried to reconstruct the third peak, at 4.3 Å, in the FT using the corresponding peak in o-Al_6Mn. About 5 Mn were found at 4.77 Å (figure 9*c*), in accordance with the 4.8 Mn at 4.8 Å obtained by neutron diffraction (Janot *et al* 1987a). This comparison between EXAFS and neutron results gives us confidence in finding some

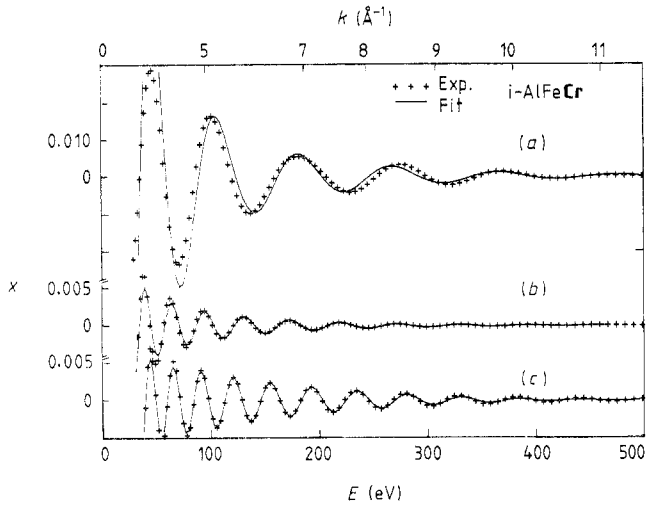

Figure 10. i–AlFeCr alloy: Fourier-filtered first (*a*), second (*b*) and third (*c*) shell on the Cr K edge (crosses) and their simulation (dashed line) as described in the text.

information by EXAFS up to 5 Å even in disordered structures, where the EXAFS signal is very small. Moreover, the large k-range ($2k_{max} \simeq 25$ Å^{-1}) spanned in the EXAFS experiments allows us to determine more precisely the first shell of neighbours and to distinguish between the different subshells.

If the short range order appears similar enough in the three non-crystalline AlMn alloys (table 1), the second and third neighbours look somewhat different. In particular, the contribution of the Mn–Mn pairs distant from 4.5 Å is more important for the T-phase than for the i-one.

6. AlFeCr alloys

6.1. Icosahedral phases

The inverse FTs of the main peak are similar enough for both Fe and Cr edges. Nevertheless, the spectrum decreases more rapidly on the Fe edge than on the Cr one. Here again an *a priori* reconstruction of the spectra was based on a Mackay icosahedron modelling. Supplementary subshells have, however, to be added as for i-AlMn (figure 10*a*) and some TM–TM pairs were also found in the first coordination shell like in i-AlCr (Sadoc *et al* 1987). This is in accordance with some recent EXAFS study performed on the Cr edge in i-$Al_6Cr_{0.7}Fe_{0.3}$ (Van Netten *et al* 1988). The σ disorder values were found to be a little smaller for the Cr central atom than for Fe (table 1), but the resulting radial distributions of the Al pairs are likewise enough around both Fe and Cr atoms (figure 11, dashed line).

For the Cr edge, the small peak at 3.7 Å was found to be due to 3 Fe/Cr at 4.45 Å (figure 10*b*) using experimental amplitudes and phase shifts extracted from α-AlMnSi. Since Fe, Mn and Cr are neighbouring elements in the periodic table, they can be confused in the EXAFS analysis. The inverse FT of the peak at 4.2 Å can be fitted using amplitudes and phase shifts extracted either from pure chromium or from o-Al_6Mn and α-AlMnSi. This yields 4 ± 1 Fe/Cr at 4.87 ± 0.05 Å plus 3.5 ± 1 Cr at 5.1 ± 0.1 Å

(figure 10*c*) and consequently 8 ± 2 atoms at an average distance 5.0 Å, which is consistent with the neutron result of six atoms at 5.0 Å. These distance values are the same as those found previously in an EXAFS study of i-AlCr (Sadoc *et al* 1987). Moreover, they correspond to the Mn–Mn distances in the Audier and Guyot (1986) model of i-AlMn. In fact, with this modelling, the second Mn neighbours of a central Mn atom consist of 5 Mn at 5.10 Å in the icosahedron of the central atom plus other Mn atoms at 4.85 Å belonging to adjacent icosahedra (figure 7). Therefore, in i-AlFeCr, the Cr atoms appear connected in the same way as the Mn ones in i-AlMn.

On the other hand, there is no distinct second- or third-neighbour peak in the FT of the Fe edge and, consequently, the environment of a Fe atom is more disordered than that of a Cr atom. As a matter of fact, it could appear as a more damped version of i-AlMn (figure 5).

6.2. Decagonal phases

As for the icosahedral phases, the first-neighbour shells of Fe and Cr atoms were found to be similar (table 1). The radial distributions of the Fe/Cr–Al pairs are asymmetrical and were simulated with two distances: 6 Al at 2.53 Å and 4 Al at 2.80 Å, with smaller σ values for the Cr central atom (figure 11, solid line). A subshell of TM–TM pairs (transition metal) was also found at ~2.61 Å as in neutron diffraction data in the same alloys (Dubois and Janot 1988, Janot *et al* 1987a). Since the σ values are smaller around a Cr atom than around a Fe one, the interatomic bonds appear to be tighter in Cr-based quasi-crystalline alloys.

The peak at 3.7 Å in the FT of the Fe edge can be reconstructed, as for decagonal AlMn, by TM–TM pairs at 4.47 Å. On the Cr edge, the peaks at 3.7 Å and 4.2 Å are not well separated and were analysed altogether using amplitudes and phase shifts extracted from o-Al_6Mn and α-AlMnSi. They were found to be due to distances of 4.5 Å, 4.87 Å and 5.0 Å. The radial distribution function (RDF) of these Cr–TM pairs has been calculated from a sum of Gaussian distributions with the R and N given by EXAFS and with σ = 0.16 Å; such a value allows us to compare our RDF with that obtained by neutron diffraction (Sadoc and Calvayrac 1986). The resulting RDF is shown in figure 12 together with the one obtained in i-AlFeCr. These RDFs consist of one double peak, the contribution of the 4.87 Å and 5.0 Å being mixed up. The variation observed in going from the i phase to the T phase is qualitatively the same as for the RDF of Janot *et al* (1987a).

The TM–TM distance of 4.47 Å, which exists in decagonal AlFeCr and AlMn alloys, appears also in o-Al_6Mn as well as in α-AlMnSi. A prominent feature of the o-Al_6Mn and α-AlMnSi structures is the layering of atoms. In o-Al_6Mn (Nicol 1953), the manganese atoms lie in sheets parallel to the (001) face at heights $c/4$ and $3c/4$ with a distance between two Mn–Mn nearest neighbours of 4.47 Å, identical to the value found in decagonal alloys. In α-AlMnSi (Cooper and Robinson 1966), the structure can also be described in terms of layers of manganese atoms about 4.45 Å apart. Moreover, the contribution of this distance is lacking or is not important in i-AlMn and in i-AlFeCr. At this point, it is tempting to suggest that a distance of 4.47 Å as observed in the decagonal phase is also due to a layering of the Mn atoms that goes along with the periodic one-dimensional stacking of 2D Penrose lattices parallel to the 10-fold axis.

7. Conclusions

We have compared the local order in periodic, quasi-periodic and non-periodic alloys. The environment of the closest neighbours is similar through the different non-crystalline

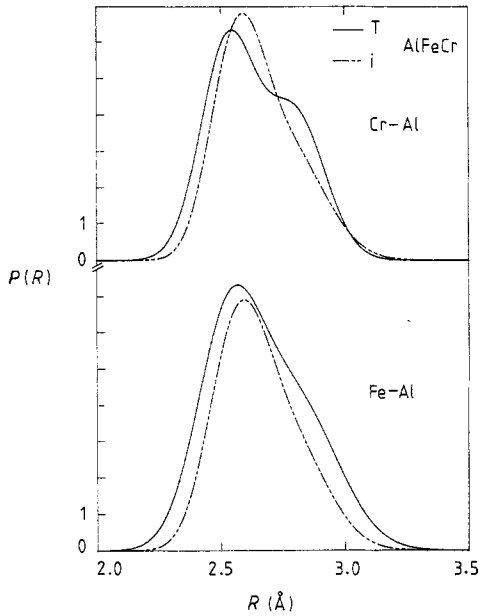

Figure 11. Fe/Cr–Al pair distribution function in icosahedral (dashed line) and decagonal (solid line) AlFeCr alloys.

phases. In the icosahedral phases, it has been interpreted starting from a Mackay icosahedron modelling, but adding supplementary subshells. Evidence for Mn–Mn close contact was found, suggesting that some fundamental rearrangement of the MI stacking must be considered. This point might be related to the short vertex–vertex distance along the triad diagonal in the oblate Penrose tiles. The magnetic behaviour of the AlMn icosahedral phases might also be related to this small number of Mn–Mn close contact pairs, but comparison with crystalline β-AlMnSi makes this interpretation rather uncertain.

On the other hand, the second and third neighbourhoods of a Mn/Fe/Cr atom are very different from one phase to another. They are highly disordered in the amorphous phase. In the icosahedral AlFeCr phase as well as in the decagonal one, they differ around a Fe atom and a Cr one. The Fe environment appears always more disordered than the Cr one and cannot be well determined.

The Fourier transforms obtained on the Mn, Fe and Cr edges and the different neighbourhood achieved around Mn, Fe and Cr atoms, could appear as a proof of the non-isomorphous substitution of Mn by Fe or Cr. However, neutron diffraction was used to check accurately the effectiveness of the random substitution of manganese for the pseudo-element FeCr. On the one hand, the intensity beneath the pseudo-Bragg peaks is, as expected, a parabolic function of the substitution rate (Janot *et al* 1987b). On the other hand, the total intensity pattern, which includes information on the disorder of the structure as well as on the irrational projection from hypercubic lattice, may be reconstructed for a given composition from a set of partial functions measured with three independent specimens (Dubois and Janot 1987, 1988, Janot *et al* 1987a). Both arguments show that the substitution is isomorphous.

Comparing neutron diffraction and EXAFS experiments, the k window applied in Fourier transforming the data is smaller for the neutron scattering ($q_{max} \simeq 16$ Å^{-1}) than

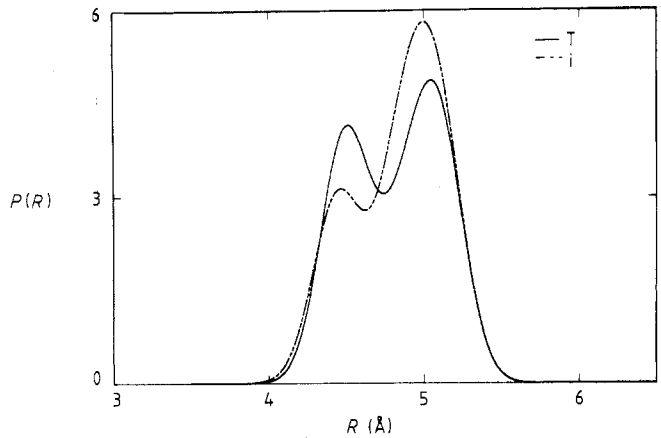

Figure 12. Radial distribution function of TM atoms around a Cr atom in icosahedral (dashed line) and decagonal (solid line) AlFeCr alloys.

for EXAFS ($2k_{max} \simeq 22$–25 Å^{-1}). The direct consequence is the broadening of the FT of the neutron data. So EXAFS is more sensitive to sharp features and to the asymmetry in the radial distribution function, while neutron better represents the whole distribution and gives the average distances (Sadoc and Calvayrac 1986). This is possibly the reason why the EXAFS and neutron diffraction results appear different.

The Cr–Cr connections were found similar to those obtained in i-AlCr (Sadoc *et al* 1987). Agreement with partial pair distribution functions deduced from neutron diffraction data was also found satisfactory. These data, however, lead to a modelling that takes into account a decoration that is not grounded on Mackay icosahedra (Janot and Dubois 1988, Janot *et al* 1988). Discussion of the difference between such various structural approaches is beyond the scope of this paper and will be given elsewhere.

In decagonal AlMn and AlFeCr alloys, we have found an important contribution of Mn–Mn and Fe–Fe pairs at 4.47 Å, a distance of second neighbours which appears in o-Al_6Mn as well as in α-AlMnSi and suggests a layering of atoms in planes perpendicular to the 10-fold axis of the decagonal phase.

Acknowledgments

We wish to thank J C Lasjaunias, Y Calvayrac, C Berger and P Sainfort for supplying samples, and J P Houin and P Weinland for technical assistance. We are grateful to the staff of the Laboratoire de l'Accélérateur Linéaire for dedicated runs at the DCI storage ring to LURE. Illuminating discussions with C Janot and J Pannetier are gratefully acknowledged.

References

Audier M and Guyot P 1986 *Phil. Mag.* B **53** L43–51
Bellissent R, Hippert F, Monod P and Vigneron F 1987 *Phys. Rev.* B **36** 5540
Bendersky L 1985 *Phys. Rev. Lett.* **55** 1461

Bendersky L, Schaefer R J, Biancaniello F S, Boettinger W J, Kaufman M J and Shechtman D 1985 *Scr. Metall.* **19** 909
Berger C, Lasjaunias J C, Tholence J L, Pavuna D and Germi P 1988a *Phys. Rev.* B **37** 6525
Berger C, Lasjaunias J C and Paulsen C 1988b *Solid State Commun.* **65** 425
Boyce J B, Bridges F G and Hauser J J 1986 *J. Physique Coll Suppl.* **47** C8 1029
Cahn J W, Gratias D and Mozer B 1988 *J. Physique* **49** 1225
Cooper M and Robinson K 1966 *Acta Crystallogr.* **6** 614
Dubois J M, Dehghan K, Chieux P and Laridjani M 1987 *J. Non-Cryst. Solids* **93** 179
Dubois J M, Dehghan K, Janot C, Chieux P and Chenal B 1985 *J. Physique* **46** C8 461
Dubois J M and Janot C 1987 *J. Physique* **48** 1981
—— 1988 *Europhys. Lett.* **5** 235
Dubois J M, Janot C and de Boissieu M 1988 *Quasicrystalline Materials, ILL/CODEST Workshop* ed. C Janot and J M Dubois (Singapore: World Scientific) p 97
Duneau M and Oguey C 1989 *J. Physique* **50** 135
Fontaine A, Lagarde P, Raoux D and Esteva J M 1979 *J. Phys. F: Met. Phys.* **9** 2143
Gratias D 1988 *Quasicrystalline Materials, ILL/CODEST Workshop* ed. C Janot and J M Dubois (Singapore: World Scientific) p 83
Janot C and Dubois J M 1988 *J. Phys. F: Met. Phys.* **18** 2303
Janot C, Dubois J M and Pannetier J 1987a *Workshop Quasicrystals, Peking* ed. K H Kuo (Switzerland: Trans. Tech.) p 329
—— 1987b *Physica* B & C **146** 351
Janot C, Dubois J M, Pannetier J, de Boissieu M and Fruchart R 1988b *Quasicrystalline Materials, ILL/CODEST Workshop* ed. C Janot and J M Dubois (Singapore: World Scientific) p 107
Lasjaunias J C, Tholence J L, Berger C and Pavuna D 1987 *Solid State Commun.* **64** 425
Lee P A and Beni G 1977 *Phys. Rev.* B **15** 2862
Lee P A and Pendry J B 1975 *Phys. Rev.* B **11** 2795
Ma Y, Stern EA and Bouldin C E 1986 *Phys. Rev. Lett.* **57** 1611
Mackay A L 1962 *Acta Crystallogr.* **15** 916
Maret M, Pasturel A, Senillou C, Dubois J M and Chieux P 1988 *J. Non-Cryst. Solids* **106** 96
Nicol A D I 1953 *Acta Crystallogr.* **6** 285
Robinson K 1952 *Acta Crystallogr.* **5** 397
Sadoc A 1986 *J. Physique Coll Suppl.* **47** C8 1003
Sadoc A and Calvayrac Y 1986 *J. Non-Cryst. Solids* **88** 242
Sadoc A, Flank A M and Lagarde P 1988a *Phil. Mag.* B **57** 399
Sadoc A, Flank A M, Lagarde P and Dubois J M 1988b *Quasicrystalline Materials, ILL/CODEST Workshop* ed. C Janot and J M Dubois (Singapore: World Scientific) p 148
Sadoc A, Flank A M, Lagarde P, Sainfort P and Bellissent R 1986 *J. Physique* **47** 873
Sadoc A, Lagarde P and Sainfort P 1987 *Int. J. Mod. Phys.* B **1** 133
Shechtman D, Blech I, Gratias D and Cahn J W 1984 *Phys. Rev. Lett.* **53** 1951
Stern E A, Sayers D E and Lytle F W 1975 *Phys. Rev.* B **11** 4836
Teo B K and Lee P A 1979 *J. Am. Chem. Soc.* **101** 2815
Van Netten T J, Schurer P J and Niesen L 1988 *J. Phys. F: Met. Phys.* **18** 1037
Wyckoff R W G 1982 *Crystal Structures* vol 1 (Malabar, FL: Krieger) p 16